18

Effect of laser treatment on the Structure and Spectral-Luminescent Properties of Graphene Dots

© E. P. Menshova, E. V. Seliverstova, N. Kh. Ibrayev

Institute of Molecular Nanophotonics, Buketov Karaganda University,
100024 Karaganda, Kazakhstan

e-mail: genia_sv@mail.ru

Received on November 30, 2021
Revised on November 30, 2021
Accepted on February 18, 2022

The structure and optical properties of nanodots based on graphene oxide (GO) obtained by ablation by laser radiation with different wavelengths were studied. It was shown that after laser ablation, the average lateral size of GO sheets decreases from 820 ± 120 nm to 204 ± 40 nm and 105 ± 23 nm for samples prepared at $\lambda_{gen} = 355$ and 532 nm, respectively. In this case, a change in the intensities of the 2D and G bands was observed, which indicates a decrease in the number of layers in the GO sheets. The optical density of GO dispersions and the intensity of fluorescence depend on the ablation conditions. After ablation, the optical density of GO increased by $\sim 13\%$ for samples obtained at $\lambda_{gen} = 355$ nm and by 20% for $\lambda_{gen} = 532$ nm. The fluorescence intensity of GO ablated at $\lambda_{gen} = 532$ nm increased by 57% relative to the value registered for GO before ablation. For 355 nm, the fluorescence intensity was changed by 7%.

Keywords: graphene oxide, graphene dots, ablation, structure, optical properties.

DOI: 10.21883/EOS.2022.05.54444.21-22

Introduction

The studies in the field of the use of graphene carbon nanostructures for the recent time have resulted in significant growth of publications devoted to synthesis and study of luminescent carbon and graphene dots. Versus conventional semiconductor quantum dots and organic pigments, photoluminescent carbon-containing dots are stable in water solutions, are chemically inert, photostable, biocompatible and low toxic [1–3].

Different authors have shown that optical properties of graphene dots depend not only on their structure and composition, but also on the production conditions. One of the methods to produce graphene dots is the laser ablation.

The method of pulse laser ablation is a single-stage, low-cost and fast method to prepare graphene dots with the controllable parameters.

In particular, this method was used in the work [4] to produce graphene oxide nanostructures. It was shown that in the process of ablation graphene oxide nanostructures are formed with various shapes: ribbon, flakes and quantum dots with simultaneous photoreduction of the graphene oxide. Quantum dots of graphene oxide have a blue photoluminescence, which is a result of recombination of the charge carriers localized on zig-zag edges. At the same time, intensity of illumination varies for the dots produced at different irradiation times.

Also, this method was used for synthesis of the graphene oxide dots in the work [5]. The diameter of the produced structures varies from 5 to 30 nm, these dots have a good stability and crystallinity. The emission spectrum of the produced nanostructures is located within the yellow-green region, which is non-typical for graphene dots. The authors have shown that these dots have high optical electronic properties and were used as the markers for visualization of cancer cells.

The works [6, 7] have shown that the efficiency of luminescence of graphene dots can be controlled, by varying the laser ablation time.

It is well known [8] that the laser ablation process efficiency directly depends not only on the laser radiation exposure time, its energy or power, but also on the generation wavelength (λ_{gen}). Match of the used λ_{gen} with the absorption band of the used substance will lead to fall of the ablation efficiency due to the energy losses. This work provides the results of the study of structural and optical properties of nano-dots based on the graphene oxide (GO), produced by laser radiation ablation with different wavelengths.

Experimental part

Single-layer graphene oxide (GO, Cheaptubes) was used for production of dispersions. GO concentration in deionized water (AquaMax) was 0.25 mg/mL. For the dispersion production the solution was ultrasonically treated during 30 min. After that, the solution was centrifugated at 6000 rpm during 1 h.

Ablation was performed with the second or the third harmonic of the solid-state Nd : YAG-laser (LQ215, SolarLS) with $\lambda_{gen} = 532$ nm and $\lambda_{gen} = 355$ nm, $\tau_{pulse} = 10$ ns with the pulse energy density equal to 120 J/cm^2. The experiment conditions were selected so that the energy density at different wavelengths of laser radiation would be the same.

The ablation time was equal to 30 min. The height of the ablated liquid was 0.8 cm. During laser ablation the dispersion was continuously mixing by means of magnetic agitator.

The GO particles size was determined by using the dynamic light scattering method by means of the Zetasizer nano S90 analyzer (Malvern). The morphology of the graphene oxide particles on the surface of silicon plates was studied by means of electron scanning microscope Mira-3 LMU (Tescan). The Raman spectra for the produced samples were registered with Confotec MR520 (3D Scanning Raman Confocal Microscope, Sol Instruments) with excitation by laser at the wavelength of 532 nm.

The absorption spectra were measured by means of the Cary-300 spectrometer (Agilent). The fluorescence was registered by means of Eclipse spectrofluorometer (Agilent). The fluorescence decay kinetics of graphene dots were measured by means of TCSPC (time-correlated single photon counting) system (Becker&Hickl) with the excitation wavelength $\lambda_{exc} = 375$ nm. The fluorescence lifetimes were evaluated by processing the decay kinetics by means of SPCImage software (Becker&Hickl) according to the procedure given in the works [9, 10]. All measurements were performed in 1 cm quartz cells at the room temperature.

Results and discussion

According to the measurements (Fig. 1), immediately after dispersion production, more than 50% of GO particles have the lateral size of 710−820 nm, each of the particle sizes 615 and 955 nm has 15 percent.

The particles of lower diameter are represented only to 10−15% of the total number of particles and have the size about 350−500 nm. After GO ablation by UV laser radiation, average size of sheets is reduced considerably to 204±40 nm. In the samples ablated at 532 nm, the average diameter of GO particles was reduced down to 105±23 nm (Fig. 1).

According to the studies of the morphology of synthesized graphene dots by means of SEM (Fig. 2), in the samples produced by radiation at $\lambda_{gen} = 532$ nm, the particles size is lower than that of GO ablated at 355 nm. Both GO sheets size reduction, and change of the layers number in them is observed for both samples. In particular, in SEM images of GO samples before ablation we can distinguish shrinks and folds appearing as a result of interlayer electrostatic interaction inside particles of GO [11, 12]. After ablation the shrinks on the samples surface are virtually invisible.

Decrease of the number of multilayer particles in dispersions of GO after ablation also was confirmed by the data of Raman spectroscopy (Fig. 3, *a*). The *D*- and *G*-stripes are manifested in Raman spectra, which are specific for graphene oxide. As can be seen from the data of Table 1, in case of ablation of GO by laser radiation at $\lambda_{gen} = 532$ nm there are no clear displacements of the maximum of *D*-, *G*- and 2*D*-stripes. After ablation at λ_{gen}=355 nm there is displacement of the scattering band maximum towards the lower frequencies region, which could indicate decrease of the number of individual double bonds that are in resonance at higher frequencies [13,14]. However, at the same time, there is change of the ratio of intensities of *D*- and *G*-bands I_D/I_G.

Table 1. Position and intensity of Raman bands of GO in dispersion after ablation at different density of the energy of laser radiation

λ_{gen}, nm	D, cm^{-1}	G, cm^{-1}	I_D/I_G	$2D$, cm^{-1}	I, r.u.	I_{2D}/I_G
before	1359	1602	0.93	2746	28602	0.65
355	1354	1598	0.93	2746	20938	0.57
532	1359	1602	0.93	2746	20285	0.56

For the case in question the ratio I_D/I_G has not changed, which indicates stability of the chemical composition of GO in case of ablation both by UV and by green light. Nevertheless, after ablation, there is change of intensities I_{2D}/I_G [13], which indicates decrease of the number of layers in the sheets of GO.

According to the definition given in [15], the graphene nano-dots refer to GO sheets with the thickness of not to exceed 5 monolayers with lateral sizes of lower than 100 nm. This condition is met for the samples produced by irradiation with light at $\lambda = 532$ nm.

The GO absorption spectra before and after ablation are given in Fig. 3, *b*. In the absorption spectrum we may distinguish the maximum at ~ 230 nm and an unclear shoulder of about 300 nm. The first band is associated with electronically excited transitions between $\pi\pi^*$-orbitals in aromatic C = C-bonds. The shoulder at 300 nm is caused by $n \rightarrow \pi^*$ transitions in C = O-bonds [11,16]. After ablation of dispersions the shape of absorption bands has not changed. Whereas the absorbance has increased by $\sim 13\%$ for the samples produced at $\lambda_{gen} = 355$ nm and by 20% for $\lambda_{gen} = 532$ nm.

The GO fluorescence spectra before ablation refer to wide stripes with the maximum at 450 nm (Fig. 4). In case of the excitation wavelength change the fluorescence maximum is not displaced. The maximum intensity of fluorescence was registered during its excitation at $\lambda_{exc} = 320$ nm.

The spectra of fluorescence of samples after ablation are within the same region of the wavelengths as for GO before ablation. For both types of GO samples the position of the fluorescence band maximum and its intensity highly depend on the λ_{exc}. The maximum intensity of fluorescence at 450 nm was registered at $\lambda_{exc} = 320$ nm, the same as for GO before ablation. During excitation at $\lambda_{exc} = 350$ nm there is bathochromic displacement of the maximum of the fluorescence spectrum at ~ 5 nm with the decrease of total intensity of the spectrum. When the spectrum of fluorescence is excited at 370 nm, then the band maximum is manifested at about 500 nm. Wherein the illumination intensity is far lower, than in the two previous cases.

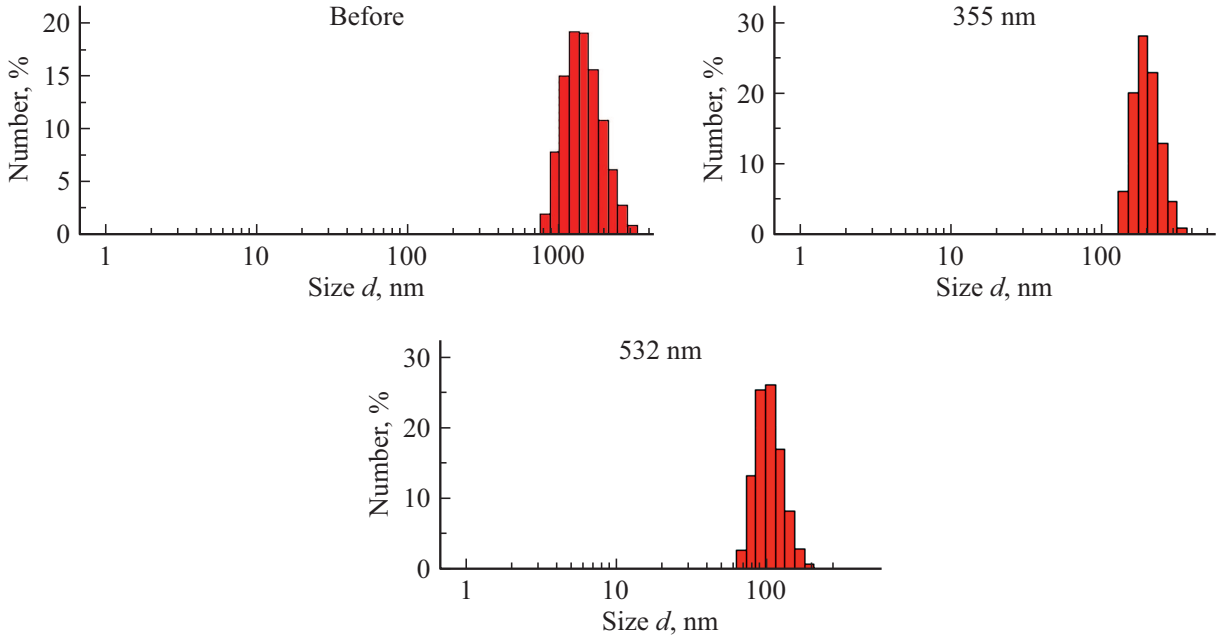

Figure 1. GO particle-size distribution in the dispersion before and after ablation at different wavelengths of laser radiation.

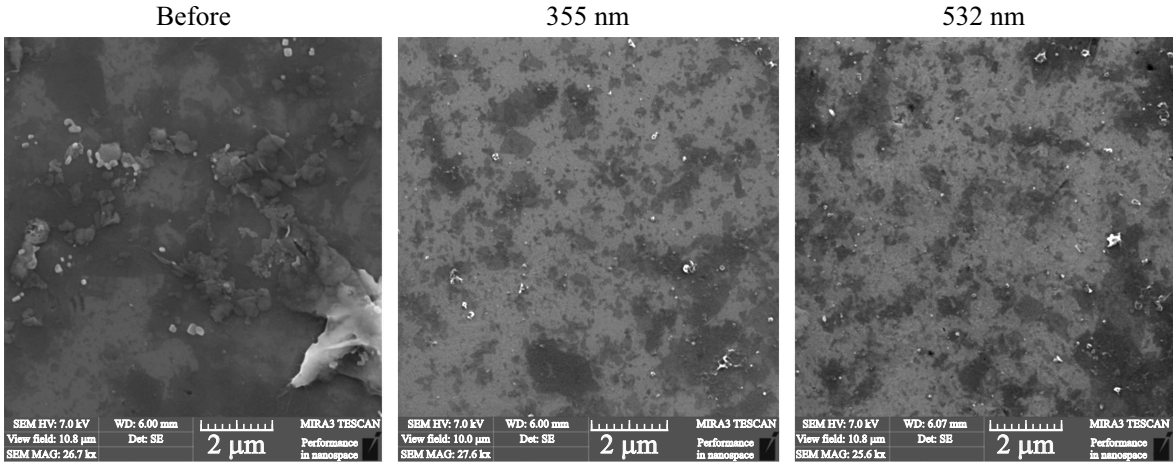

Figure 2. SEM images of GO before and after ablation at different wavelengths of laser radiation.

It should be noted that the luminescent capacity of GO is higher, when the dispersion is ablated at $\lambda_{gen} = 532$ nm. Thus, the intensity of fluorescence has increased by 57% relative to the value registered for GO before ablation. For 355 nm the fluorescence intensity has fallen only by 7%. It could be associated with the fact that during ablation at 355 nm the light is generally absorbed by GO, therefore, as can be seen above, the size of particles after ablation is higher, than in case of the use of laser radiation at $\lambda_{gen} = 532$ nm.

According to the measured spectra of fluorescence excitation (on tab in Fig. 4, *a*), main contribution into GO illumination is from the sites actively absorbing the light in the region of 320–340 nm. After laser ablation the excitation spectrum does not change its shape. Excitation of luminescence at 250 nm resulted in a low fluorescence within blue-green region of the spectrum.

The GO fluorescence lifetime before and after ablation is given in Table 2. The fluorescence decay curves are described quite good by the biexponential expression, which indicates the presence of at least two fluorescence sources. According to the data, after ablation, the average fluorescence lifetime (τ_{av}) is rising. It occurs due to a higher portion of contribution and the growth of long-term component into the total fluorescence kinetics.

Today, the mechanism of fluorescence occurrence in graphene nanostructures remains poorly studied, however, the majority of the authors believe [15,17,18] it may be

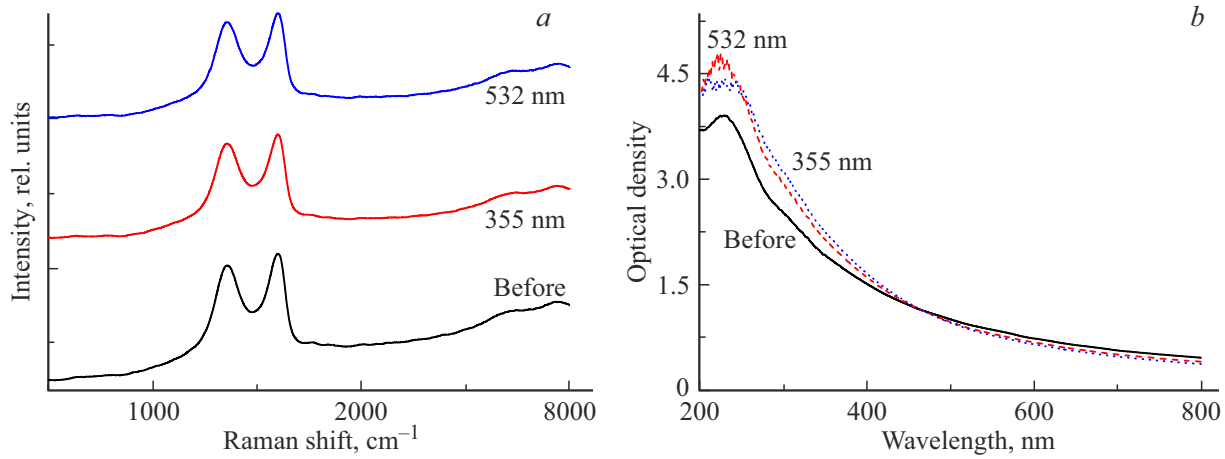

Figure 3. Raman (a) and absorption (b) spectra of GO before and after ablation at different wavelengths of laser radiation.

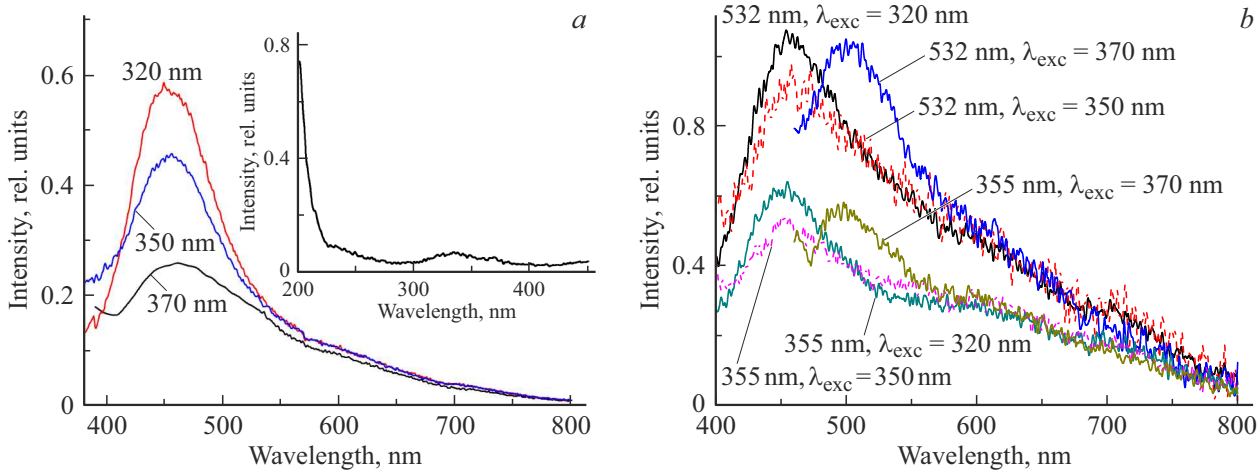

Figure 4. Spectra of fluorescence of GO before (a) and after (b) ablation at different wavelengths of laser radiation and at λ_{exc}. The tab (a) provides the GO excitation spectra before ablation at $\lambda_{reg} = 460$ nm.

Table 2. GO fluorescence lifetime before and after ablation at different wavelengths of laser radiation

λ_{gen}, nm	τ_1, ns	A, %	τ_2, ns	A, %	τ_{av}, ns
before	0.34	92.0	2.71	8.0	0.53
355	0.32	92.0	2.80	12.0	0.63
532	0.30	79.0	3.10	21.0	0.89

attributed to different radiating groups or localized electron-hole couples because of isolation of sp^2-clusters inside sp^3-matrix.

Conclusion

In this way we have studied the effect of the laser radiation wavelength used in ablation of GO for its structural and optical properties. After laser ablation, average lateral size of GO sheets is reduced from 820±120 nm to 204±40 nm and 105±23 nm for the samples made at $\lambda_{gen} = 355$ and 532 nm, accordingly. The data on the sizes of nano-dots of GO, produced by the dynamic light scattering method, are confirmed by the sizes obtained from SEM images.

The studies of structural properties by the Raman spectroscopy have shown that after ablation there is change of the intensities I_{2D}/I_G, which indicates decrease of the number of layers in sheets of GO [13]. Wherein, these changes are more notable for the samples produced at $\lambda_{gen} = 532$ nm. According to the measurements, there are no remarkable displacements of the maximum of D-, G- and $2D$-bands. After ablation at $\lambda_{gen} = 355$ nm there is displacement of the maximum of scattering bands towards the lower frequencies region.

Absorbance of the produced GO solutions and intensity of their fluorescence depend on the ablation conditions. In the absorption spectrum of GO we may distinguish the maximum at ~ 230 nm and an unclear shoulder of about 300 nm. After ablation of dispersions the shape of

absorption bands has not changed. Whereas the absorbance has increased by $\sim 13\%$ for the samples produced at $\lambda_{gen} = 355$ nm and by 20% for $\lambda_{gen} = 532$ nm.

The maximum of the GO dispersion fluorescence spectrum before ablation falls within 450 nm and does not depend on the photoexcitation wavelength. The maximum intensity of fluorescence varies based on the excitation wavelength. After ablation, both the position and the intensity of fluorescence depend on λ_{exc}. At that, the luminescent capacity of GO is higher, when the dispersion is ablated at $\lambda_{gen} = 532$ nm. In particular, the intensity of fluorescence has increased by 57% relative to the value registered for GO before ablation. For 355 nm the fluorescence intensity has fallen only by 7%. It could be associated with the fact that during ablation at 355 nm the light is generally absorbed by GO, therefore, as can be seen above, the size of particles after ablation is higher, than in case of the use of laser radiation at $\lambda_{gen} = 532$ nm.

The fluorescence decay kinetics are approximated by the biexponential expression, which indicates the presence of two illumination sources. After ablation, the average fluorescence lifetime τ_{av} is rising. It occurs due to a higher portion of contribution and the growth of long-lived component into the total luminescence kinetics.

The obtained results can be used for creation of organic luminescent materials, optical nano-technologies, as well as in photovoltaics, biophysics and bioimaging.

Funding

This work was carried out within the framework of the research grant AP08052672, funded by the Ministry of Education and Science of the Republic of Kazakhstan.

Conflict of interest

The authors declare that they have no conflict of interest.

References

[1] H-M.F. Murilo, S. Rodrigo, A.M. Luiza, S.C. Daniel. Environ. Sci.: Nano., **7** (12), 3710 (2020). DOI: 10.1039/D0EN00787K
[2] M.R. Younis, G. He, J. Lin, H. Peng. Front. Chem., **8**, 424 (2020). DOI: 10.3389/fchem.2020.00424/
[3] P. Tian, L. Tang, K.S. Teng, S.P. Lau. Mater. Today Chem., **10**, 221 (2018). DOI: 10.1016/j.mtchem.2018.09.007
[4] T.N. Lin, K.H. Chih, C.T. Yuan, J.L. Shen, C.A.J. Lince, W.R. Liud. Nanoscale, **7,** 2708 (2015). DOI: 10.1039/C4NR05737F
[5] S. Kang, K.M. Kim, K. Jung, Y. Son, S. Mhin, J.H. Ryu, K.B. Shim, B. Lee, H. Han, T. Song. Sci. Rep., **9**, 4101 (2019). DOI: 10.1038/s41598-018-37479-6
[6] E. Seliverstova, N. Ibrayev, E. Menshova. Fullerenes, Nanotubes, Carbon Nanostruct., **30** (1), 119 (2021). DOI: 10.1080/1536383X.2021.1984899
[7] E. Seliverstova, N. Ibrayev, E. Menshova, E. Alikhaidarova. Mater. Res. Express, **8** (11), 115601 (2021). DOI: 10.1088/2053-1591/ac31fc
[8] Yu.S. Tveryanovich, A.A. Manshina, A.S. Tverjanovich. Russ. Chem. Rev., **81** (12), 1091 (2012). DOI: 10.1070/RC2012v081n12ABEH004285
[9] E.V. Seliverstova, D.A. Temirbayeva, N.Kh. Ibrayev, A.A. Ishchenko. Theor. Exp. Chem., **55**, 115 (2019). DOI: 10.1007/s11237-019-09602-9
[10] E.V. Seliverstova, N.Kh. Ibrayev, G.S. Omarova, A.A. Ishchenko, M.G. Kucherenko. J. Lumin., **235**, 118000 (2021). DOI: 10.1016/j.jlumin.2021.118000
[11] E.V. Seliverstova, N.K. Ibrayev, R.K. Dzhanabekova. Russ. J. Phys. Chem. A, **91**, 1761 (2017). DOI: 10.1134/S003602441709028X
[12] L.J. Cote, F. Kim, J.X. Huang. J. Am. Chem. Soc., **131**, 1043 (2009). DOI: 10.1021/ja806262m
[13] A. Jorio, R. Saito, G. Dresselhans, M.S. Dresselhaus G.F. *Raman spectroscopy in graphene related systems* (Wiley-VCH, Verlag, 2011). DOI:10.1002/9783527632695
[14] J.I. Paredes, R.S. Villar, F.P. Solis, A.A. Martinez, J.M. Tascon. Langmuir, **25**, 5957 (2009). DOI: 10.1021/la804216z
[15] S. Zhu, Y. Song, X. Zhao, J. Shao, J. Zhang, B. Yang. Nano Res., **8** (2), 355 (2015). DOI: 10.1007/s12274-014-0644-3
[16] E.A. Ganash, G.A. Al-Jabarti, R.M. Altuwirqi. Mater. Res. Express, **7** (1), 015002 (2020). DOI: 10.1088/2053-1591/ab572b
[17] Sh. Lai, Yo. Jin, L. Shi, R. Zhou, Yu. Zhou, D. An. Nanoscale, **12**, 591 (2020). DOI: 10.1039/C9NR08461D
[18] Q. Mei, B. Liu, G. Han, R. Liu, M.-Yo. Han, Zh. Zhang. Adv. Sci., **6** (14), 1900855 (2019). DOI: 10.1002/advs.201900855